Electronic Supplementary Material (ESI) for Chemical Communications

Supplementary information

Flexible and robust MoS_2/graphene hybrid paper cross-linked by a polymer ligand: a high-performance anode material for thin film lithium-ion batteries

Yi-Tao Liu [a], *Xiao-Dong Zhu* [b], *Zhi-Qiang Duan* [a] *and Xu-Ming Xie* [a*]

[a]Key Laboratory of Advanced Materials (MOE), Department of Chemical Engineering, Tsinghua University, Beijing 100084, China

[b]Academy of Fundamental and Interdisciplinary Sciences, Harbin Institute of Technology, Harbin 150080, China

[*] Corresponding author.

E-mail address: xxm-dce@mail.tsinghua.edu.cn

S1. Experimental details

S1.1 Raw materials

MoS_2 was purchased from Sigma-Aldrich. GO was purchased from Nanjing XF Nano. PEO (M_w = 100,000) was purchased from Alfa Aesar. $CuCl_2 \cdot 2H_2O$ and DMF were purchased from Beijing Chemical Works. Hydrazine hydrate was purchased from Guangdong Chemical Reagent Engineering-Technological Research and Development Centre.

S1.2 Preparation of a MoS_2/DMF solution

The procedures for exfoliating MoS_2 into nanosheets were adapted from a previous report [1]. Briefly, the MoS_2 powder was added to DMF at an initial concentration of 10 mg mL^{-1}, homogenized at 11,500 rpm for 60 min, and then subjected to cup-horn sonication at 300 W for 60 min. The obtained slurry was centrifuged at 1,500 rpm for 45 min, and the top 1/2 supernatant was collected. The collected supernatant was further centrifuged at 3,000 rpm for another 45 min. The precipitated solid was collected and re-dispersed in DMF by sonication, yielding a dark green MoS_2/DMF solution (0.2 mg mL^{-1}) containing relatively large MoS_2 nanosheets (Fig. 1).

S1.3 Preparation of a GO/DMF solution

To produce a GO/DMF solution [2], GO was directly added to DMF at an initial concentration of 0.2 mg mL^{-1}, and then subjected to gentle sonication at 100 W for 60 min. The obtained GO/DMF solution was brilliant yellow, and could stand for weeks without obvious precipitates (Fig. S2).

S1.4 Preparation of freestanding MoS_2/r-GO paper cross-linked by PEO

The MoS_2 and GO/DMF solutions were mixed, and PEO was added at different MoS_2/GO/PEO wt ratios

(9/0/1, 7/2/1, 6/3/1 and 5/4/1). A small amount of dehydrated $CuCl_2$ was added to the MoS_2/GO/PEO system, which was then kept under magnetic stirring for 24 h. After coordination hydrazine hydrate was added, and the MoS_2/GO/PEO system was kept at 80 ^oC for 12 h such that GO was sufficiently reduced to *r*-GO. It was reported that GO could be chemically reduced to *r*-GO by hydrazine hydrate, which would re-stack and thus precipitate from DMF [3]. However, the MoS_2/GO/PEO system could be successfully converted to the MoS_2/*r*-GO/PEO system by hydrazine hydrate without obvious precipitates (Fig. S7), thanks to the steric stabilisation effect of PEO which facilitated the following liquid-phase processing. The vacuum filtration was employed to obtain a piece of flexible and robust MoS_2/*r*-GO paper chemically cross-linked by PEO, which was peeled off the poly(vinylidene fluoride) (PVDF) membrane by soaking in acetone (Fig. S8). Note that if the PEO fraction was too low, it was helpless to create flexible and robust MoS_2/*r*-GO/PEO paper; if the PEO fraction was too high, it would impose an adverse effect on the electrochemical performance of the MoS_2/*r*-GO/PEO paper due to the decreased electronic conductivity resulting in increased internal resistance and charge transfer [4]. Moreover, it should be mentioned that the higher the *r*-GO content, the stronger the MoS_2/*r*-GO/PEO paper. The MoS_2/*r*-GO/PEO (9/0/1) paper was the most fragile, which would at least partially lead to the poor cycle stability.

S1.5 Preparation of a film anode for the electrochemical testing

The freestanding MoS_2/*r*-GO paper could be tailored arbitrarily by scissors without cracking, and directly attached to a copper foil with a layer of silver paste (Fig. S9). The layer of silver paste was aimed to improve the surface roughness of the copper foil, and thus to increase the efficiency of physical contact between the film anode and the current collector (copper foil) [5]. The film anode was then dried in nitrogen at 120 ^oC for 12 h to adequately evaporate the residual organic solvent, and equipped in a CR2032 coin cell according to the configuration of (-) Li | electrolyte | freestanding MoS_2/*r*-GO/PEO film anode (+) with a liquid electrolyte (1 M solution of $LiPF_6$ in ethylene carbonate–dimethyl carbonate at a vol ratio of 1 : 1) in an

argon-filled glove box. A Celgard 2400 membrane was used as the separator.

S1.6 Equipment

TEM was performed by a Hitachi H7700 operated at an accelerating voltage of 100 kV. HRTEM was performed by a JEOL JEM-2010 operated at an accelerating voltage of 120 kV. SEM was performed by a Tescan VEGA3 at an accelerating voltage of 20 kV. Raman spectra were recorded by a Renishaw RM2000 spectrometer with 514 nm laser excitation. UV-vis spectra were recorded by a Pgeneral TU-1810 twin-beam spectrometer within a wavelength range of 200–900 nm. FTIR spectra were recorded by a Nicolet 560 spectrometer. XPS spectra were recorded by an Escalab 250 Xi spectrometer.

S2. UV-vis spectrum of a MoS_2/DMF solution

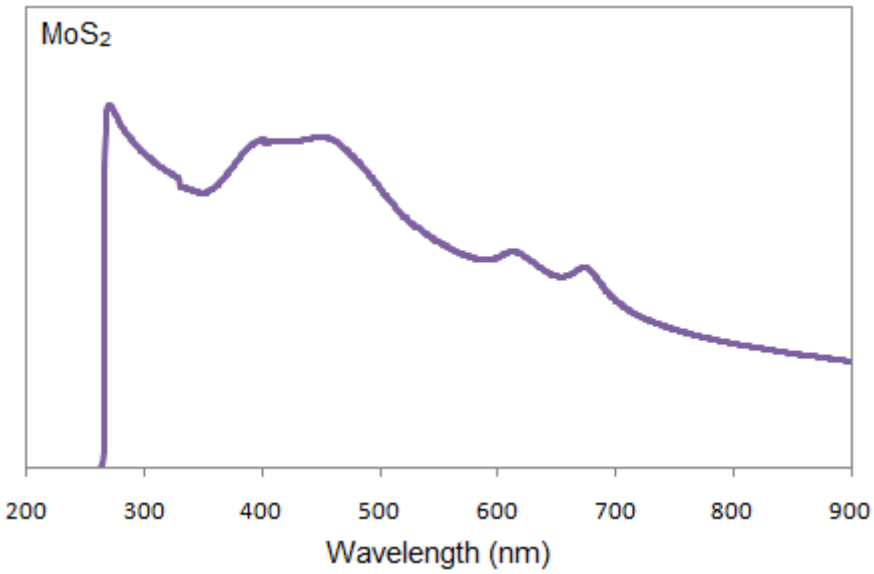

Fig. S1 UV-vis spectrum of a MoS_2/DMF solution within a wavelength range of 200–900 nm. The spectrum shows two well-resolved characteristic peaks, *i.e.*, A_1 at 673 nm and B_1 at 613 nm, within 600–700 nm. The two peaks are the first (n = 1) members of two excitonic Rydberg series that are associated with the direct transition and their energy separation can be ascribed to the spin-orbit splitting of the top of the valence band at the K point [6]. The presence of peaks A_1 and B_1 in the UV/vis spectrum demonstrates the successful exfoliation of MoS_2 into nanosheets in DMF.

S3. Photograph and TEM image of GO/DMF solution

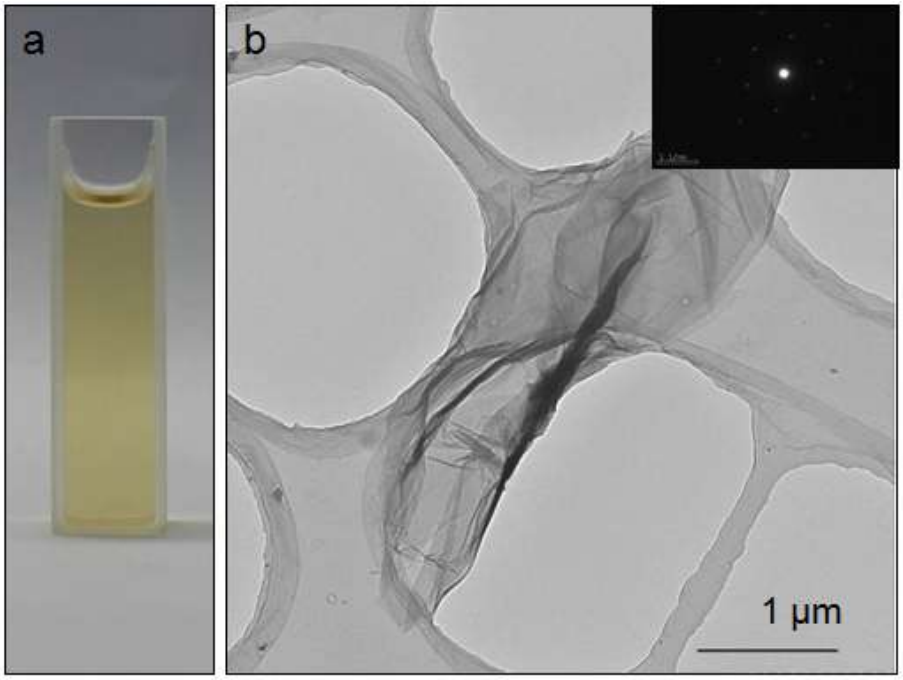

Fig. S2 (a) Photograph of a brilliant yellow GO/DMF solution; (b) TEM image of a large-area, highly crumpled GO nanosheet and the corresponding ED pattern (insert).

S4. UV-vis spectrum of a GO/DMF solution

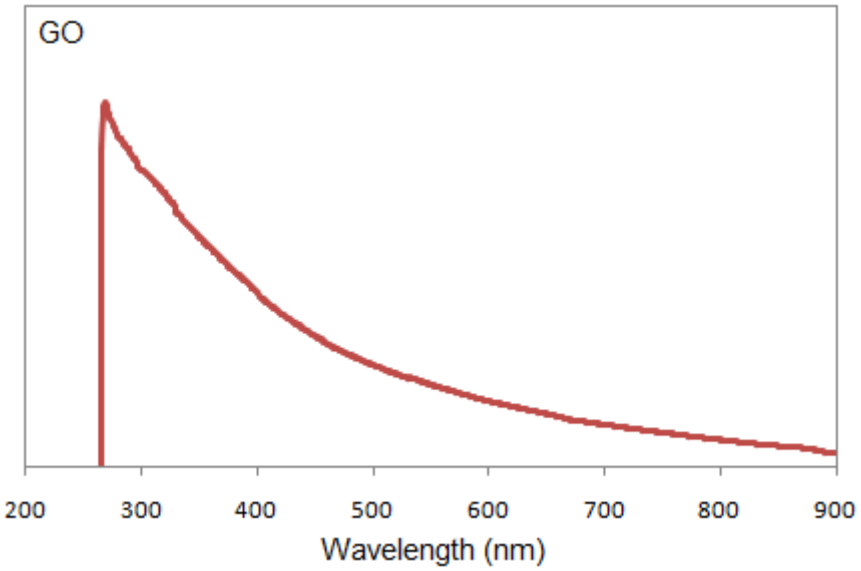

Fig. S3 UV-vis spectrum of a GO/DMF solution within a wavelength range of 200–900 nm. Generally, there should be two characteristic peaks, *i.e.*, a maximum at ~230 nm, presumably due to the π→π* transition of the C–C bonds; a shoulder at ~300 nm, presumably due to the n→π* transition of the C=O bonds [2]. However, the two peaks are invisible because the data within 200–280 nm cannot be collected because DMF has strong absorption in that wavelength range.

S5. Photograph of a MoS_2/GO/PEO system before and after coordination

Fig. S4 Photograph of a MoS_2/GO/PEO (6/3/1) system before (left) and after (middle) coordination, and a MoS_2/GO (6/3) system after coordination for comparison (right).

S6. FTIR spectra of a MoS_2/GO/PEO system before and after coordination

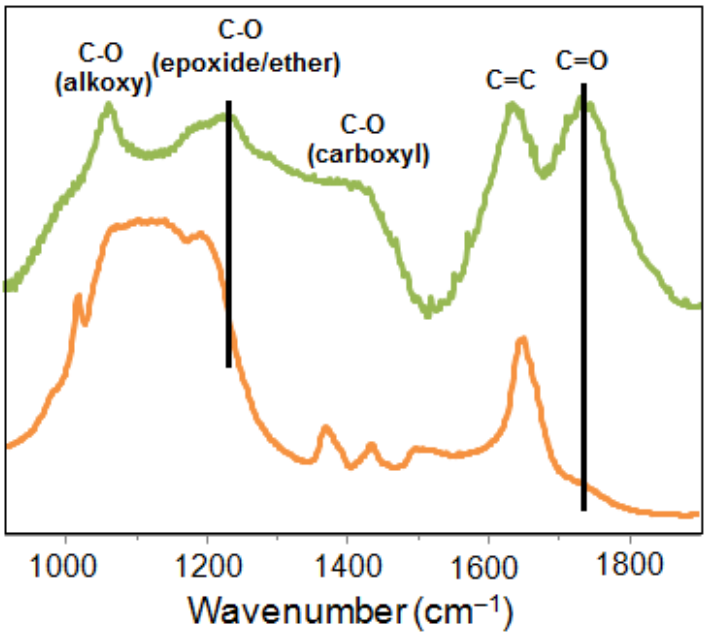

Fig. S5 FTIR spectra of a MoS_2/GO/PEO system (6/3/1) before (green) and after (orange) coordination. Since the FTIR spectrum of MoS_2 is featureless within the wavenumber range of 500–3000 cm^{-1}, the characteristic peaks mainly arise from GO. Clearly, before coordination the FTIR spectrum has five characteristic peaks, *i.e.*, C=O bonds (carboxyl/carbonyl) at 1734 cm^{-1}, C=C bonds (aromatic ring) at 1647 cm^{-1}, C–OH bonds (carboxyl) at 1414 cm^{-1}, C–O bonds (epoxide/ether) at 1216 cm^{-1}, and C–O bonds (alkoxy) at 1090 cm^{-1}. After coordination, the C=O (carboxyl/carbonyl) peak is nearly invisible, and the C–OH (carboxyl) peak increases significantly, indicating the successful coordination between C=O bonds and Cu^{2+} ions. Besides, the C–O (epoxide/ether) peak also disappears, suggesting the possible ring-opening coordination between the C–O bonds and Cu^{2+} ions [7]. This result is in accord with the XPS result shown in Fig. 2.

S7. Raman spectra of a coordinated MoS_2/GO/PEO system before and after reduction

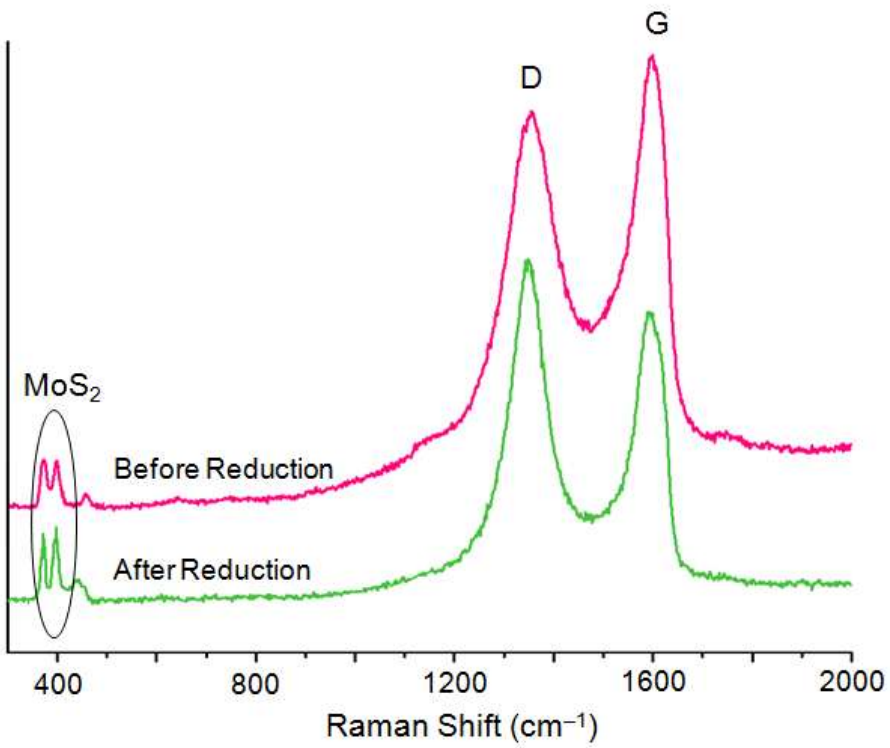

Fig. S6 Raman spectra of a coordinated MoS_2/GO/PEO (6/3/1) system before (green) and after (red) reduction. Before reduction, the Raman spectrum of the coordinated MoS_2/GO/PEO system has four characteristic peaks. The two weaker ones at 381 and 407 cm^{-1} correspond to the in-plane E_{2g} and out-of-plane A_{1g} vibrations of MoS_2, respectively [8]. The two stronger ones at 1351 and 1584 cm^{-1} correspond to the D and G peaks of GO, respectively [9]. After reduction, the D/G intensity ratio increases significantly, suggesting the a decreased average size of the sp^2 domains upon the reduction of GO to *r*-GO. This phenomenon is ascribed by Ruoff *et al.* to the creation of new graphitic domains after reduction, which are smaller in the size but larger in the number [10].

S8. Photograph of coordinated MoS_2/r-GO/PEO systems

Fig. S7 Photograph of three coordinated MoS_2/*r*-GO/PEO systems (7/2/1, 6/3/1 and 5/4/1).

S9. Photographs of freestanding MoS_2/r-GO/PEO (6/3/1) hybrid paper

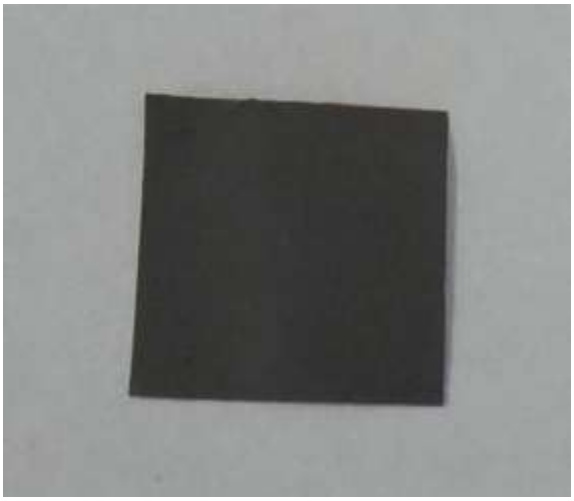

Fig. S8 Photograph of a piece of freestanding MoS_2/*r*-GO/PEO (6/3/1) hybrid paper peeled off the PVDF membrane and tailored arbitrarily by scissors.

Fig. S9 Photograph of a naked copper foil (left) and a copper foil attached with the tailored freestanding MoS_2/*r*-GO/PEO (6/3/1) hybrid paper (right). Note that there is still scope for improving the electrochemical performance of our film anode by, *e.g.*, rationally reducing its thickness to shorten the diffusion pathways, or trying to further optimise its composition.

S10. SEM image of a MoS_2/GO hybrid directly cross-linked by Cu^{2+} ions (without PEO)

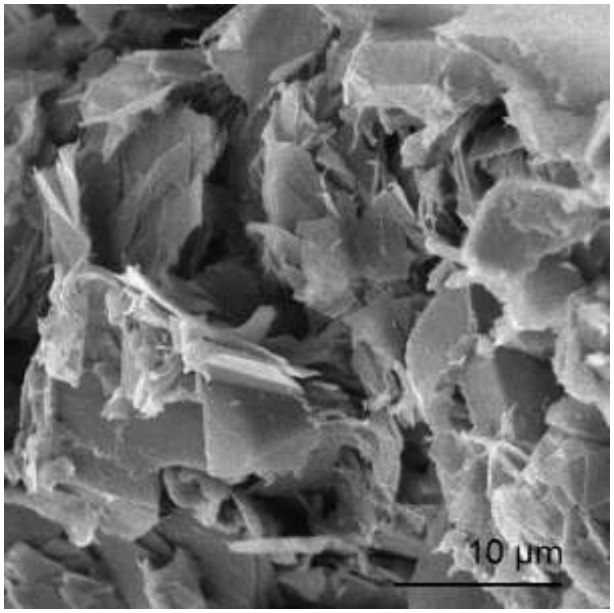

Fig. S10 SEM image of a MoS_2/GO hybrid directly cross-linked by Cu^{2+} ions (without PEO).

S11. Supplementary references

[1] J. N. Coleman, M. Lotya, A. O'Neill, S. D. Bergin, P. J. King, U. Khan, K. Young, A. Gaucher, S. De, R. J. Smith, I. V. Shvets, S. K. Arora, G. Stanton, H.-Y. Kim, K. Lee, G. T. Kim, G. S. Duesberg, T. Hallam, J. J. Boland, J. J. Wang, J. F. Donegan, J. C. Grunlan, G. Moriarty, A. Shmeliov, R. J. Nicholls, J. M. Perkins, E. M. Grieveson, K. Theuwissen, D. W. McComb, P. D. Nellist and V. Nicolosi, *Science*, 2011, **331**, 568.

[2] J. I. Paredes, S. Villar-Rodil, A. Martínez-Alonso and J. M. D. Tascón, *Langmuir*, 2008, **24**, 10560.

[3] S. Park, J. An, I. Jung, R. D. Piner, S. J. An, X. Li, A. Velamakanni and R. S. Ruoff, *Nano Lett.*, 2009, **9**, 1593.

[4] J. Xiao, D. Choi, L. Cosimbescu, P. Koech, J. Liu and J. P. Lemmon, *Chem. Mater.*, 2010, **22**, 4522.

[5] T. Yuan, B. Zhao, R. Cai, Y. Zhou and Z. Shao, *J. Mater. Chem.*, 2011, **21**, 15041.

[6] J. P. Wilcoxon, P. P. Newcomer and G. A. Samara, *J. Appl. Phys.*, 1997, **81**, 7934.

[7] S. Park, K.-S. Lee, G. Bozoklu, W. Cai, S. T. Nguyen and R. S. Ruoff, *ACS Nano*, 2008, **2**, 572.

[8] C. Lee, H. Yan, L. E. Brus, T. F. Heinz, J. Hone and S. Ryu, *ACS Nano*, 2010, **4**, 2695.

[9] M. S. Dresselhaus, A. Jorio, M. Hofmann, G. Dresselhaus and R. Saito, *Nano Lett.*, 2010, **10**, 751.

[10] S. Stankovich, D. A. Dikin, R. D. Piner, K. A. Kohlhaas, A. Kleinhammes, Y. Jia, Y. Wu, S. T. Nguyen and R. S. Ruoff, *Carbon*, 2007, **45**, 1558.